

A Novel Compact Electromagnetic Band Gap Structure to Reduce the Mutual Coupling in Multilayer MIMO Antenna

Kompella S. L. Parvathi^{1, *}, Sudha R. Gupta^{1, *}, and Pramod P. Bhavarthe²

Abstract—This paper presents a novel compact multilayer meander strip line step-via electromagnetic band-gap (MLSV-EBG) structure with the application of mutual coupling reduction in a multilayer multiple input multiple output (MIMO) antenna. The proposed EBG-cell has been developed by using multilayer, novel meander strip line, and step-via concept. To analyse the proposed EBG a parallel LC model method is used. In the proposed MLSV-EBG structure, due to step-via concept, current path length increases, and compactness is achieved per unit cell. Parametric study is also presented. MLSV-EBG structure unit cell is simulated using ANSYS high frequency structure simulator (HFSS), and 5×5 cells are printed on an FR4 substrate for band-gap measurements. Simulated and measured results prove that compared with three-layer central located via EBG (CLV-EBG) and edge located via EBG (ELV-EBG), size reductions of 47.01% and 43.01% have been achieved, respectively, which shows that step via concept gives the significant size reduction per unit multilayer EBG cell. The application of proposed MLSV-EBG for the reduction of mutual coupling between two multilayer MIMO antennas is also demonstrated. The key contribution of the presented work is that the proposed compact multi-layer EBG structure is useful in a multi-layer environment at a lower frequency.

1. INTRODUCTION

Electromagnetic band gap (EBG) structures play an important role in antenna and microwave engineering due to their stopband characteristics [1, 2]. In past years, single layer [3–5], polarization dependent [6, 7], multi-layer [8–16] type of EBG structures have been reported. As per recent trends in antenna and microwave engineering multi-layer EBG structures are in demand [8–16]. A dual layer EBG (DL-EBG) structure [8] is proposed to develop two element and four element miniaturized microstrip patch antennas at 2.5 GHz. The patch size of DL-EBG is $0.041\lambda_{2.5\text{GHz}}$. Two layer edge located via and interdigital EBG (TELI-EBG) [9] is reported with EBG patch size of $0.083\lambda_{5.0\text{GHz}}$ to reduce the in band radar cross section (RCS) of a dual band microstrip patch antenna array. Electromagnetic bandgap (EMBG) [10] is proposed for microstrip band-stop filter design in S-band with EBG patch size $0.105\lambda_{2.25\text{GHz}}$. Multilayer EBG (M-EBG) [11] is introduced for on package antenna isolation and simultaneous switching noise (SSN) in high speed digital circuits with EBG patch size $0.056\lambda_{7.50\text{GHz}}$. A four layer interleaved electromagnetic bandgap (IL-EBG) [12] is investigated for SSN application. The size of each IL-EBG patch is $0.042\lambda_{3.2\text{GHz}}$. An S-shaped two layer EBG [13] is proposed to reduce the mutual coupling between two patch antennas with periodic size of $0.120\lambda_{5.3\text{GHz}}$. A four layer electromagnetic EBG (ML-EBG) [14] is proposed to reduce mutual coupling of a multiple input multiple output (MIMO) antenna at 2.55 GHz. Out of four layers, in three layers air is used as the substrate with EBG patch size of $0.119\lambda_{2.55\text{GHz}}$. However, the reported multi-layer EBG structures are limited to give a simple structure [8–12] and compact size [9–11, 13, 14].

Received 18 May 2020, Accepted 9 July 2020, Scheduled 23 July 2020

* Corresponding author: Kompella S. L. Parvathi (k.radhakumari@somaiya.edu).

¹ Electronics Department, K. J. Somaiya College of Engineering, Vidyavihar, University of Mumbai, Mumbai, India. ² Department of Electronics and Telecommunication Engineering, VPP College of Engineering, Sion, University of Mumbai, Mumbai, India.

The major contribution of this paper is a novel compact multilayer meander strip line step-via electromagnetic band-gap (MLSV-EBG) structure. In the proposed EBG structure, compactness is achieved by increasing the inductance of parallel LC with the novel concept of step via with meander line. The novel step via with meander line concept is presented in Section 2 with the simulation of unit cell of the proposed multi-layer meander stripline step-via EBG (MLSV-EBG) structure in eigenmode solution of ANSYS HFSS. In Section 3, simulation and fabricated 5×5 cells of MLSV-EBG, and band-gap measurements using suspended microstrip line method (SML) have been explained, and also MLSV-EBG is compared with the reported multilayer EBG structures. The application of MLSV-EBG to reduced mutual coupling of three layer MIMO antenna is also presented in Section 4. The paper is concluded by comparing the mutual coupling due to EBG structure in terms of isolation level (dB) and spacing between two patches with the existing work.

2. PROPOSED MULTI-LAYER MEANDER LINE STEP VIA-EBG

The conventional center located via EBG (CLV-EBG) structure can be represented as an equivalent parallel LC resonance circuit [1–4, 6–8]. The resonance frequency (f_c) of parallel LC circuit is given as

$$f_c = \frac{1}{2\pi\sqrt{LC}} \quad (1)$$

Inductance (L) and capacitance (C) are given as [2, 8]

$$L = \mu_0 h \quad (2)$$

and

$$C = \frac{a\epsilon_o(\epsilon_r + 1)}{\pi} \cosh^{-1} \left(\frac{2a + g}{g} \right) \quad (3)$$

where (μ_0) = permeability of free space, (h) = total substrate height, (a) = width of each EBG patch, (g) = gap between two adjacent EBG cells, (ϵ_r) = dielectric constant of the substrate, and (ϵ_0) = permittivity of free space. The bandgap bandwidth (BW) [1–4, 6–8] of EBG structure is given as

$$\text{BW} = \frac{\Delta\omega}{\omega} \quad (4)$$

where η is the free space impedance. (C) is due to the gap between two EBG patches and (L) due to the current path from via-ground-plane-via of the adjacent cell. From Eq. (1), in order to achieve compactness in terms of periodic size of EBG cell, the product of LC should be increased. From Eq. (2), for multi-layer or single-layer EBG [8], increasing the value of (L) is quite difficult because its value depends on (h). In order to get compactness for the multi-layer EBG structure, the path which gives the (L) should be increased.

The proposed three-layer MLSV-EBG structure evolution and unit cell geometry are shown in Figure 1 and Figure 2, respectively. Layer-1 consists of an edge located via with meander stripline-1 printed on the top of layer-1. Layer-2 consists of the center via, and meander strip line-2 is printed on the top of the layer similar to layer-1. Layer-3 consists of another edge via with a square EBG patch at the top of the layer as shown in Figure 2 and Figure 3, and meander strip line-1 and -2 give current path between via-1 and via-3 through via-2 as shown in Figure 3(a). The equivalent (C_0) and (L_0) for MLSV-EBG structure are shown in Figure 3(b). (C_0) is formed due to the fringing effect between two adjacent MLSV-EBG cells. (L_0) is due to the current path along via-3, meander strip line-2, via-2, meander strip line-1, via-1, ground plane, and adjacent MLSV-EBG cells. For the proposed MLSV-EBG, (L_0) is given by

$$L_0 = \mu_0(h_1 + h_2 + h_3 + S + S) = \mu_0(h + 2S) \quad (5)$$

where $S = S_2 + S_3 + 2S_4 + S_5 + S_6 + 2S_7$, (h_1) = layer-1 height, (h_2) = layer-2 height, (h_3) = layer-3 height, (h) = total substrate height, and (S) = total length of each meander strip line. To verify the band-gap properties of the proposed three layer MLSV-EBG, unit cell is simulated in the eigen mode of ANSYS HFSS [17]. The dispersion diagram based on the rectangular (irreducible) Brillouin zone [4] for MLSV-EBG is demonstrated in Figure 4. The parameters of the MLSV-EBG structure are taken

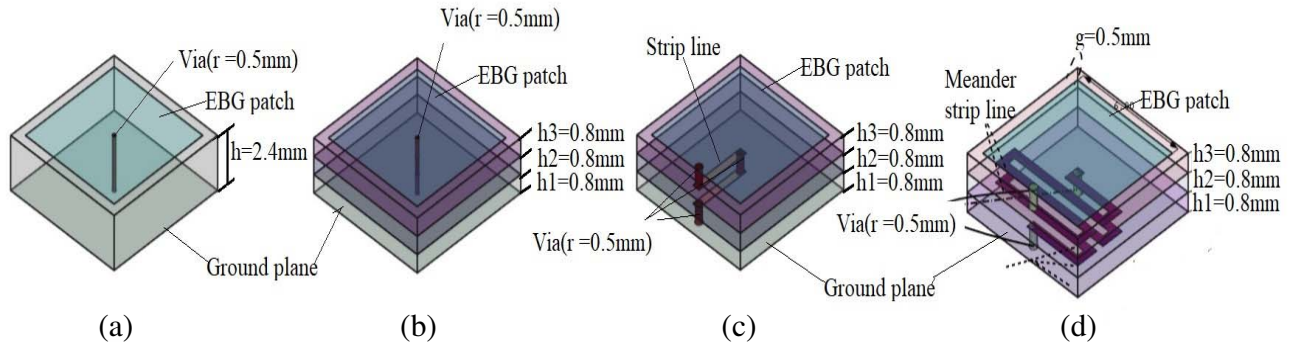


Figure 1. Evolution of proposed three-layer meander strip line step-via electromagnetic band-gap (MLSV-EBG) structure. (a) Center located via EBG (CLV-EBG), (b) three layer CLV-EBG, (c) three layer step via EBG, (d) proposed MLSV-EBG.

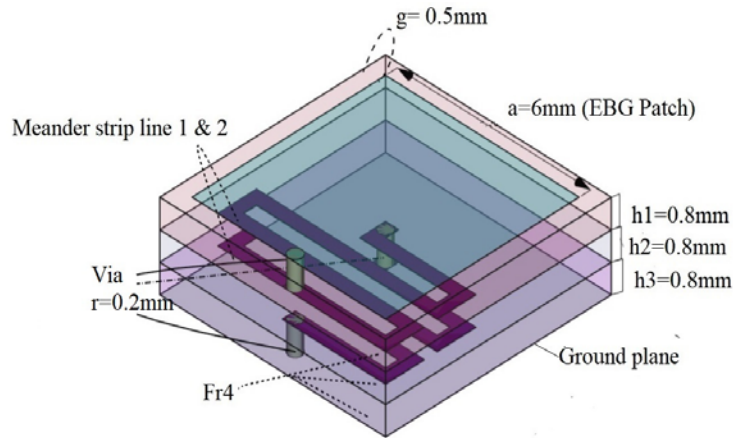


Figure 2. Geometry of the proposed three-layer meander strip line step-via electromagnetic band-gap (MLSV-EBG) structure unit cell.

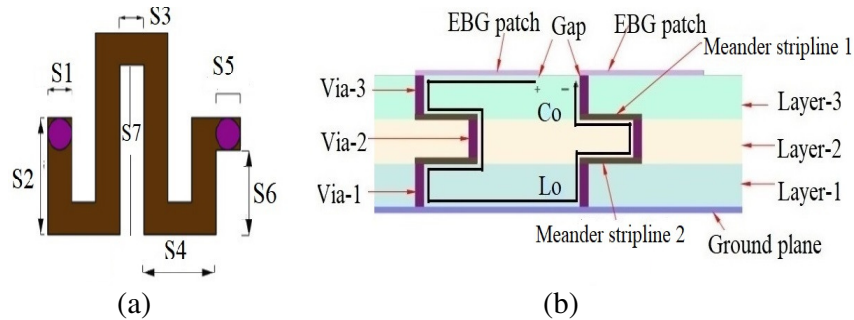


Figure 3. (a) Geometry of the each meander strip line, and (b) side view and equivalent LC circuit model of the proposed three-layer MLSV-EBG structure.

as: dielectric constant of each layer (ϵ_r) = 4.4, height of each layer (h_1) = (h_2) = (h_3) = 0.8 mm, total height of the substrate (h) = 2.4 mm, dielectric loss tangent = 0.02, and other parameters of the MLSV-EBG are mentioned in the Figure 4. From the dispersion diagram of MLSV-EBG as shown in Figure 4, frequency band-gap is observed between mode-1 and mode-2 with band-gap center frequency (f_c) at 1.64 GHz. Band gap is with lower cutoff frequency (f_l) = 1.52 GHz and higher cutoff frequency

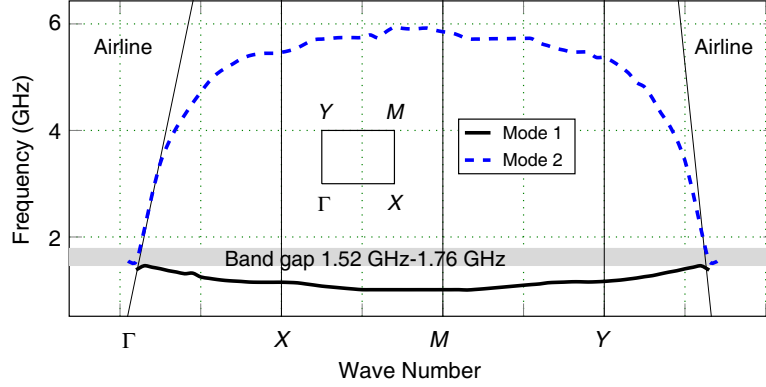


Figure 4. Dispersion diagram of proposed three-layer MLSV-EBG structure with $(a, g, r, s_1, s_2, s_3, s_4, s_5, s_6, s_7, h_1, h_2, h_3, \epsilon_r) = (6 \text{ mm}, 0.5 \text{ mm}, 0.2 \text{ mm}, 0.4 \text{ mm}, 1.45 \text{ mm}, 0.4 \text{ mm}, 1.2 \text{ mm}, 0.4 \text{ mm}, 1.05 \text{ mm}, 2.1 \text{ mm}, 0.8 \text{ mm}, 0.8 \text{ mm}, 0.8 \text{ mm}, 4.4)$.

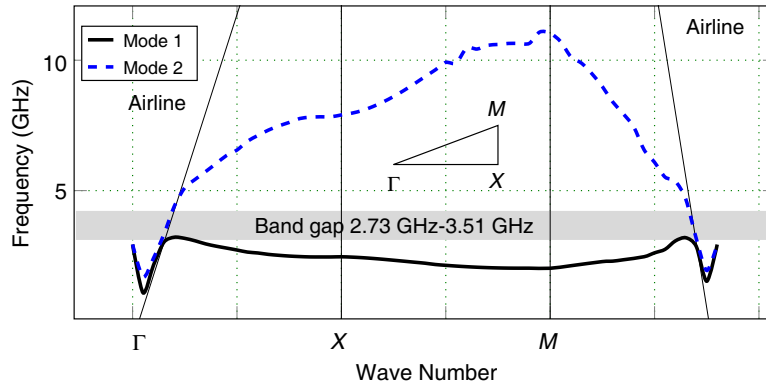


Figure 5. Dispersion diagram of three-layer CLV-EBG structure with $(a, g, r, h_1, h_2, h_3, \epsilon_r) = (6 \text{ mm}, 0.5 \text{ mm}, 0.2 \text{ mm}, 0.8 \text{ mm}, 0.8 \text{ mm}, 0.8 \text{ mm}, 4.4)$.

$(f_h) = 1.76 \text{ GHz}$. In order to compare the bandgap properties of MLSV-EBG with CLV EBG, three layer CLV-EBG is also simulated with the same parameters of the MLSV-EBG as mentioned in Figure 5. In CLV-EBG, a via is located at the center of each layer without any strips. The dispersion diagram of three layer CLV-EBG is shown in Figure 5. From the dispersion diagram of CLV-EBG, frequency band-gap is observed between mode-1 and mode-2 with (f_c) at 3.12 GHz with lower cutoff frequency $(f_l) = 2.73 \text{ GHz}$ and higher cutoff frequency $(f_h) = 3.51 \text{ GHz}$. From Eq. (4), due to an increase in the equivalent values of L and C of proposed MLSV-EBG, less band gap bandwidth is observed than three-layer CLV-EBG [1].

3. OPTIMIZATION AND EXPERIMENTAL RESULTS

To study and analyze the effect of total length of meander strip line-1 and -2 and number of substrate layers on band-gap center frequency (f_c) , 5×5 MLSV-EBG has been simulated using ANSYS HFSS. The array is developed on a three-layer substrate with $\epsilon_r = 4.4$, dielectric loss tangent = 0.02, and height of each layer = 0.8 mm using suspended microstrip line (SML) method [3] with other parameters of the MLSV-EBG mentioned earlier. (f_c) with band gap bandwidth for different total lengths of meander line with three layers of MLSV-EBG is given in Table 1.

By increasing the meander strip line length, (f_c) of MLSV-EBG is potentially reduced. As the meander strip line length increases, equivalent (L_o) and (C) also increase, and therefore, band gap bandwidth is reduced with low rejection level [1, 3]. With variation of the total length of meander strip

Table 1. Effect of total length of each meander strip line of proposed MLSV-EBG on band gap bandwidth (BW) and band gap center frequency (f_c) (for three layer MLSV-EBG).

Meander line length (mm)	BW (%)	f_c (GHz)	Patch Size
6.1	15.4	1.74	$0.034\lambda_c$
7.6	13.79	1.59	$0.031\lambda_c$
11.4	11.76	1.36	$0.027\lambda_c$
14.4	10.4	1.19	$0.023\lambda_c$
17.4	7.4	1.08	$0.021\lambda_c$

Table 2. Effect of number of layers (N) of proposed MLSV-EBG on band gap bandwidth (BW) and band gap center frequency (f_c).

N	f_l (GHz)	f_h (GHz)	BW (%)	f_c (GHz)	Patch Size
2	1.72	1.98	14.59	1.85	$0.037\lambda_c$
3	1.37	1.56	13.01	1.46	$0.029\lambda_c$
4	1.19	1.35	11.81	1.27	$0.025\lambda_c$
5	1.05	1.18	11.65	1.11	$0.022\lambda_c$

line-1 and -2, (f_c) of the MLSV-EBG is varied without changing the periodic size. This frequency variation capability of the multilayer MLSV-EBG structure is very useful in many microwave and antenna applications. In order to study the effect of number of substrate layers (N) with uniform substrate height (h) = 0.8 mm of MLSV-EBG on (f_c) and band gap bandwidth, different numbers of layers are also simulated with SML method as given in Table 2. As the number of substrate layers increases, equivalent (L) and (C) also increase, and therefore, (f_c) is also reduced with lower band gap bandwidth [1].

In order to validate the simulation results and demonstrate the bandgap of the MLSV-EBG structure, 5×5 cells [3] are printed on a three layer FR4 substrate with $\epsilon_r = 4.4$, loss tangent = 0.02, and height of each layer = 0.8 mm using suspended microstrip line (SML) [3] method in x and y directions (rectangular symmetry). Other parameters of MLSV-EBG are the same as mentioned in the earlier section. The 50Ω microstrip line is printed on a 0.8 mm substrate with $\epsilon_r = 4.4$, loss tangent = 0.02 and placed on the EBG surface. The Agilent N9923A network analyzer with the highest measurable frequency of 6 GHz is used in the measurement. Photographs of the prototype and measured (S_{12}) of MLSV-EBG in x - and y -directions are demonstrated in Figure 6. The measured results agree well with the simulated ones. The difference between simulated and measured results is due to the air gap between the layers, fabrication error, joining of the SMA connector, etc. [23]. Band gap is observed in both x - and y -directions from 1.41 GHz to 1.61 GHz ($S_{12} < -20$ dB [3]) with band gap center frequency 1.51 GHz. In stopband, some ripples are observed because of the multipath reflection effects [3]. 5×5 three layer CLV-EBG [2] and ELV-EBG [4] cells with the same geometric and substrate parameters are also fabricated for comparison. Photographs and measured (S_{12}) of CLV-EBG and ELV-EBG are shown in Figure 6. For CLV-EBG, the center frequency of bandgap is observed at (f_c) = 2.85 GHz with (f_l) = 2.52 GHz and (f_h) = 3.16 GHz, where as for ELV-EBG, the frequency of bandgap is observed at (f_c) = 2.65 GHz with (f_l) = 2.43 GHz and (f_h) = 2.89 GHz ($S_{12} < -20$ dB). The band gap bandwidth and rejection level of proposed MLSV-EBG structure are reduced due to higher equivalent inductance and capacitance value than CLV-EBG and ELV-EBG structures [1]. From simulated and experimental results, the major contribution of this work is to propose a step via concept in a multilayer EBG structure which results in size reduction of per unit cell of EBG. The proposed multilayer MLSV-EBG results in lowering the (f_c) by 47.01% and 43.01% compared to CLV-EBG and ELV-EBG structures, respectively. The comparison of the multilayer MLSV-EBG and other multilayer EBG structures is presented in Table 3.

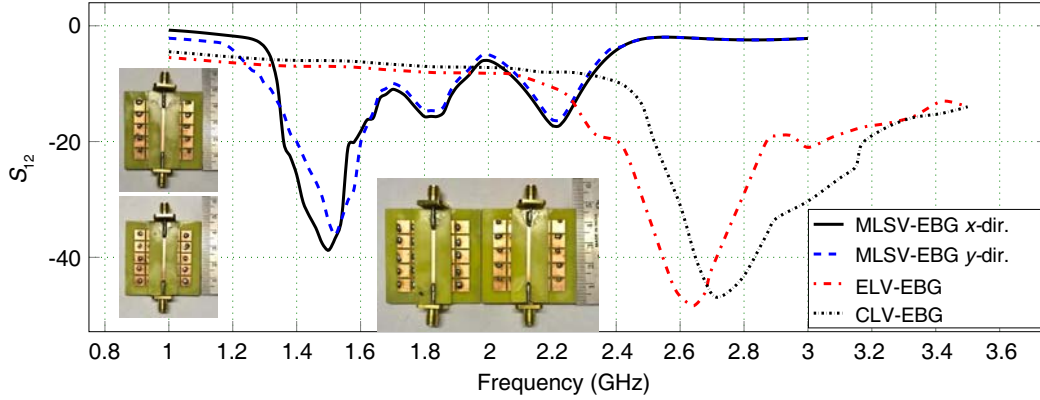


Figure 6. Photograph, and measured S_{12} using suspended microstrip line method for proposed three-layer MLSV-EBG, CLV-EBG, and ELV-EBG.

Table 3. Total number of layer (N), dielectric constant (ϵ_r), total substrate height (h), band-gap center frequency (f_c), band-gap bandwidth (in %), patch size of proposed MLSV-EBG and other multi-layer EBG structure.

Ref.	EBG	N	ϵ_r/h (mm)	f_c (GHz)	BW (%)	Patch Size
[2]	CLV EBG	3	4.4/2.4	2.85	22.45	$0.057\lambda_c$
[4]	ELV-EBG	3	4.4/2.4	2.65	17.35	$0.053\lambda_c$
[9]	TELI-EBG	2	2.65/2	5.00	10.00	$0.083\lambda_c$
[10]	EMBG	2	3.38/1.625	2.25	9.7	$0.105\lambda_c$
P. E.	MLSV-EBG	3	4.4/2.4	1.51	13.24	$0.030\lambda_c$

P. E. = Proposed EBG

4. APPLICATION

An application of the proposed MLSV-EBG structure to reduce the mutual coupling in MIMO antenna is presented in this section. In a patch antenna array, mutual coupling depends on the substrate dielectric constant, substrate thickness, and the distance between patches [18–27]. In a multilayer patch antenna array the effect of mutual coupling is more due to the increase in the height of substrate. Strong mutual coupling is present in the E -plane compared to the H -plane probe feed patch antenna [22]. There are different methods to reduce the mutual coupling of a multilayer patch antenna array. As concluded in [22], an effective method to reduce the mutual coupling is by inserting the EBG between the two patch antennas. Geometries of the two multilayer rectangular probe feed patch antennas (MRPPAs) with and without MLSV-EBG are shown in Figure 7. The parameters of MRPPA are taken as follows: dielectric constant $\epsilon_r = 4.4$, height of each layer ($h_1 = h_2 = h_3 = 0.8$ mm, dielectric loss tangent = 0.02, and other parameters are mentioned in Figure 7.

From simulated and measured results as shown in Figure 8, it is observed that -23.90 dB mutual coupling is present at 5.80 GHz [21]. To reduce the mutual coupling of the MRPPA, two columns of MLSV-EBG are inserted between MRPPAs as shown in Figure 7 with other parameters of the MLSV-EBG. The Agilent N9923A network analyzer with the highest measurable frequency of 6.00 GHz is used in the measurement. Simulated and measured results for MRPPA with MLSV-EBG are presented in Figure 9. The measured results agree well with the simulated ones. From Figure 9, it is observed that the mutual coupling is reduced by 10.81 dB at 5.80 GHz. The mutual coupling between the two elements can be studied using surface current distribution. Port 1 of the MIMO antenna is fed while port 2 is terminated with a matched load. Current distributions at 5.80 for MRPPAs with and without MLSV-EBG are shown in Figure 10. The radiation efficiency of the MRPPA with MLSV-EBG with port 1 or 2 excited is shown in Figure 11(a), and good radiation efficiency is observed over the operating

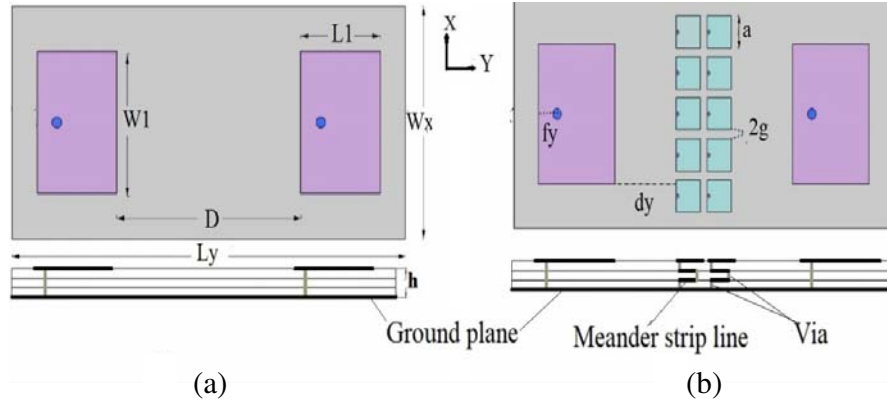


Figure 7. Top and side view of multilayer rectangular probe feed patch antennas (a) without MLSV-EBG, and (b) with MLSV-EBG with $(W_x, L_y, W_1, L_1, f_y, D, d_y, a, g, r, s_1, s_2, s_3, s_4, s_5, s_6, s_7, h_1, h_2, h_3, h) = (25.00 \text{ mm}, 55.00 \text{ mm}, 15.42 \text{ mm}, 11.04 \text{ mm}, 2.72 \text{ mm}, 25.86 \text{ mm}, 8.93 \text{ mm}, 3.5 \text{ mm}, 0.5 \text{ mm}, 0.2 \text{ mm}, 0.4 \text{ mm}, 0.75 \text{ mm}, 0.1 \text{ mm}, 0.9 \text{ mm}, 0.05 \text{ mm}, 0.35 \text{ mm}, 0.7 \text{ mm}, 2.4 \text{ mm})$.

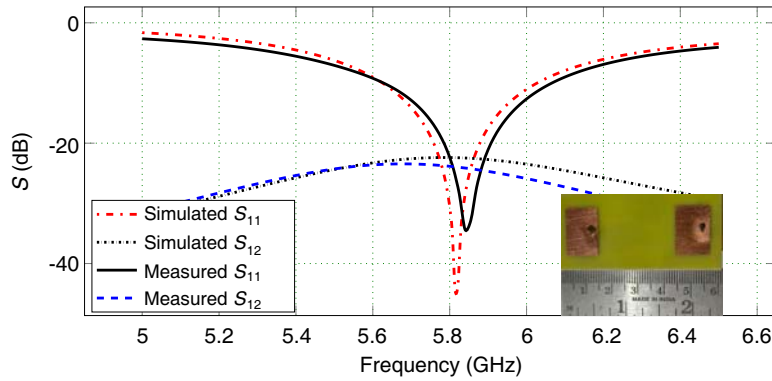


Figure 8. Photograph, simulated, and measured results of three layer rectangular probe feed patch antennas without MLSV-EBG.

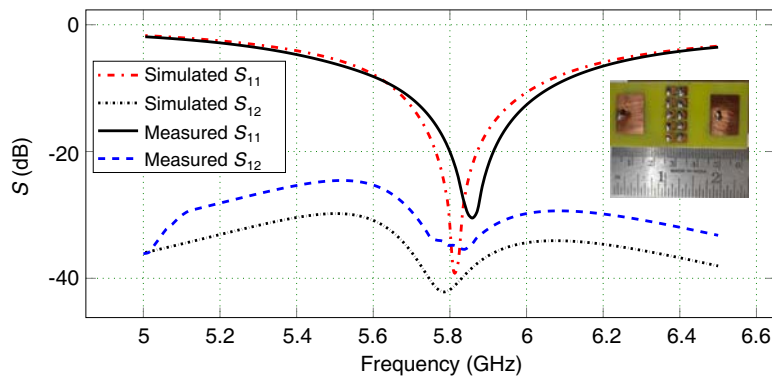


Figure 9. Photograph, simulated, and measured results of three layer rectangular probe feed patch antennas with MLSV-EBG.

bandwidth. The two port envelope correlation coefficient (ECC) is an important parameter for the antenna used for MIMO application. The ECC can be given using the method given in [28].

$$\rho_e = \frac{|S_{11}^* S_{12} + S_{21}^* S_{22}|^2}{(1 - |S_{11}|^2 - |S_{21}|^2)(1 - |S_{22}|^2 - |S_{12}|^2)} \quad (6)$$

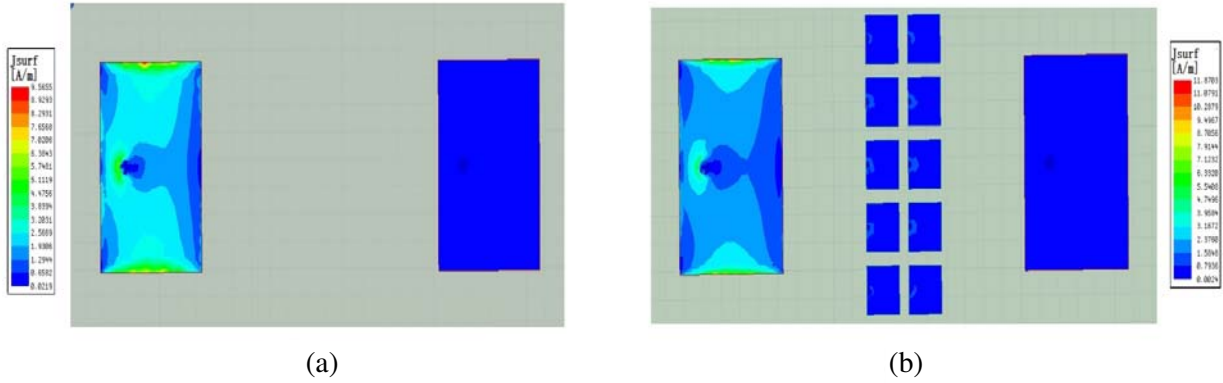


Figure 10. Surface current distribution at 5.80 GHz for MRPPA (a) without MLSV-EBG, (b) with MLSV-EBG.

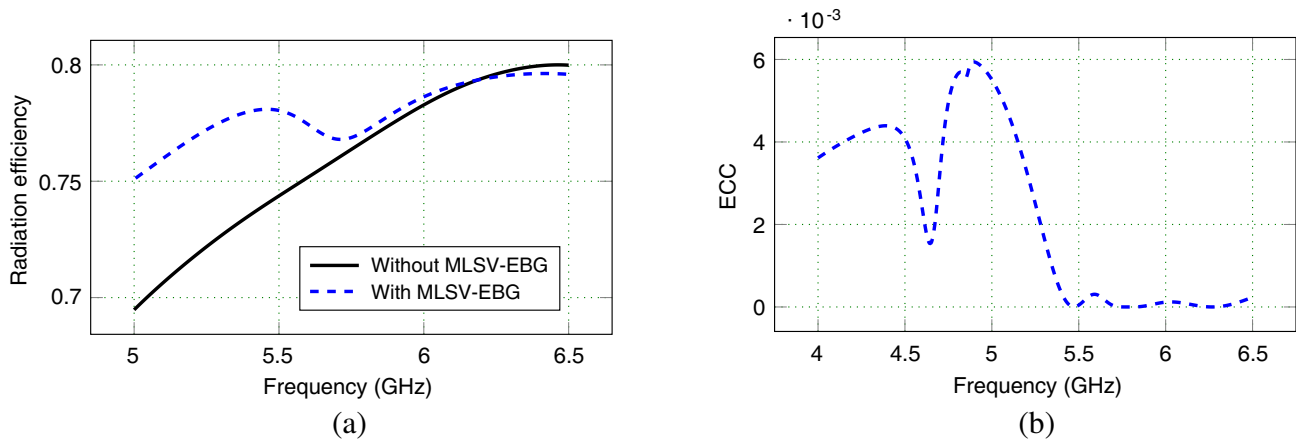


Figure 11. (a) Radiation efficiency, and (b) correlation coefficient of MRPPA.

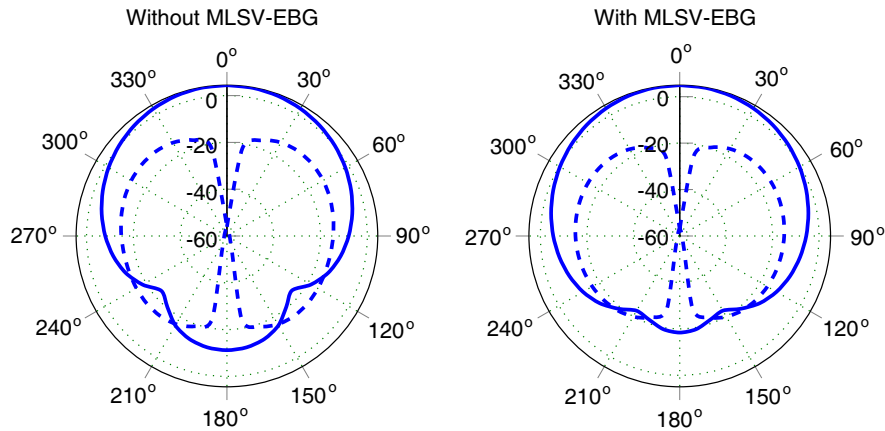


Figure 12. Radiation pattern of the MRPPA with and without MLSV-EBG at 5.80 GHz (--- Cross Polarization, — Co polarization.).

It is considered that significant diversity is achieved if the ECC is less than 0.5 [28]. ECC calculated using S parameters of the presented MRPPA with MLSV-EBG is shown in Figure 11(b). ECC less than 0.002 is achieved throughout the band which is significantly less than the ECC required for good diversity performance. Figure 12 presents the 2-D co-polarization and cross-polarization radiation patterns of the

Table 4. Comparison of mutual coupling due to EBG structure in terms of isolation level (dB), and spacing between two patch.

Ref.	EBG type	ϵ_r total sub. height h (mm)	Isolation level (dB)	Spacing between two patch
[21]	TVS-EBG	5.8/1.6	$\approx \geq 7.1$ dB at 5.8 GHz	$0.5\lambda_0$
[22]	EBG	5.8/1.92	$\approx \geq 8.00$ dB at 5.8 GHz	$0.75\lambda_0$
[29]	S-EBG	3.48/2.286	≥ 10.30 dB at 2.4 GHz	$0.84\lambda_0$
[30]	EC-EBG	4.4/2.00	≥ 4.00 dB at 5.6 GHz	$0.98\lambda_0$
[31]	Meander line	3.67/N.M.	≥ 15.51 dB at 5.29 GHz	$0.5\lambda_0$
[32]	UC-EBG	10.2/2.54	≥ 10.00 dB at 5.75 GHz	$0.63\lambda_0$
[33]	H-CELC	2.67/1.5	≥ 9.74 dB at 3.5 GHz	$\lambda_0/8.08$
[34]	Spiral EBG	2.65/2.00	≥ 6.00 dB at 3.25 GHz	$0.48\lambda_0$
PW	MLSV-EBG	4.4/2.4	≥ 10.81 dB at 5.8 GHz	$0.49\lambda_0$

P. W. = Proposed Work, N. M. = Not Mentioned

MRPPA without and with MLSV-EBG at 5.8 GHz. From radiation pattern it is clear that the proposed MSLV-EBG presents less effect on radiation pattern of the MRPPA. The comparison of mutual coupling due to EBG structure in terms of isolation level (dB) and spacing between two patches is presented in Table 4, which proves that the proposed MSLV EBG is useful for antenna and microwave engineering in multilayer environment at low frequency application.

5. CONCLUSION

In this paper, based on resonant LC circuit model a novel compact multilayer meander strip line step-via EBG (MLSV-EBG) structure is proposed. The size of unit cell of the proposed EBG structure is $0.030\lambda \times 0.030\lambda \times 0.010\lambda$ at the resonance frequency. The measured results using suspended microstrip line method shows good agreement with simulation ones. Compared to three-layer CLV-EBG and ELV-EBG, MLSV-EBG gives size reductions of 47.01% and 43.01%, respectively due to meander strip line step-via concept. The application of the proposed MLSV-EBG structure to reduce the mutual coupling between two multilayer rectangular probe feed patch antennas is also presented. Simulated and measured results prove that proposed MLSV-EBG structure is a good candidate for multi-layer applications where compactness is highly desirable.

REFERENCES

1. Yang, F. and Y. Rahmat-Samii, *Electromagnetic Band Gap Structures in Antenna Engineering*, Cambridge Univ. Press, Cambridge, U.K., 2009.
2. Sievenpiper, D., L. Zhang, R. F. J. Broas, N. G. Alexopolous, and E. Yablonovitch, "High impedance electromagnetic surfaces with a forbidden frequency band," *IEEE Trans. Microw. Theory Tech.*, Vol. 47, No. 11, 2059–2074, 1999.
3. Yang, L., M. Fan, F. Chen, J. She, and Z. Feng, "A novel compact electromagnetic-bandgap (EBG) structure and its application for microwave circuits," *IEEE Trans. Microw. Theory Tech.*, Vol. 53, No. 1, 183–190, 2005.
4. Rajo-Iglesias, E., L. Inclan-Sanchez, J.-L. Vazquez-Roy, and E. Garcia-Munoz, "Size reduction of Mushroom-type EBG surfaces by using edge-located vias," *IEEE Microw. Wireless Compon. Lett.*, Vol. 17, No. 9, 670–672, 2007.
5. Cheng, H. R., Q. Song, Y.-C. Guo, X.-Q. Chen, and X.-W. Shi, "Design of a novel EBG structure and its application in fractal microstrip antenna," *Progress In Electromagnetics Research C*, Vol. 11, 81–90, 2009.

6. Han, Z.-J., W. Song, and X.-Q. Sheng, "Gain enhancement and RCS reduction for patch antenna by using polarization-dependent EBG surface," *IEEE Antennas Wireless Propag. Lett.*, Vol. 16, 1631–1634, 2017.
7. Bhavarthe, P. P., S. S. Rathod, and K. T. V. Reddy, "A compact two via hammer spanner-type polarization-dependent electromagnetic-bandgap structure," *IEEE Microw. Wireless Compon. Lett.*, Vol. 28, No. 4, 284–286, 2018.
8. Ghosh, S., T.-N. Tran, and T. Le-Ngoc, "Dual-layer EBG-based miniaturized multi-element antenna for MIMO systems," *IEEE Trans. Antennas Propag.*, Vol. 62, No. 8, 3985–3997, 2014.
9. Zhang, S., "Novel dual-band compact HIS and its applications of reducing array in-band RCS," *Microw. Opt. Technol. Lett.*, Vol. 58, No. 3, 700–704, 2016.
10. Yang, N., Z. N. Chen, Y. Y. Wang, and M. Y. W. Chia, "A two-layer compact electromagnetic bandgap (EBG) structure and its applications in microstrip filter design," *Microw. Opt. Technol. Lett.*, Vol. 37, No. 1, 62–64, 2003.
11. Bantavis, P., M. Le Roy, A. Perennec, R. Lababidi, and D. Le Jeune, "Miniaturized wide-and dual-band multilayer electromagnetic bandgap for antenna isolation and on-package/PCB noise suppression," *IEEE 22nd Workshop on Signal and Power Integrity (SPI)*, 1–4, Brest, France, 2018.
12. Wang, C.-D. and T.-L. Wu, "Model and mechanism of miniaturized and stop band-enhanced interleaved EBG structure for power/ground noise suppression," *IEEE Trans. Electromagn. Compat.*, Vol. 55, No. 1, 159–167, 2013.
13. Veeramani, A., A. S. Arezomand, J. Vijayakrishnan, and F. B. Zarrabi, "Compact S-shaped EBG structures for reduction of mutual coupling," *IEEE Fifth International Conference on Advanced Computing Communication Technologies*, 21–25, Haryana, India, 2015.
14. Jiang, T., T. Jiao, and Y. Li, "A low mutual coupling MIMO antenna using periodic multi-layered electromagnetic band gap structures," *Appl. Comput. Electromagn. Soc. J.*, Vol. 33, No. 3, 305–311, 2018.
15. Azarbar, A. and J. Ghalibafan, "A compact low-permittivity dual-layer EBG structure for mutual coupling reduction," *International Journal of Antennas and Propagation*, Vol. 2011, 1–6, 2011.
16. Nadeem, I. and D.-Y. Choi, "Study on mutual coupling reduction technique for MIMO antennas," *IEEE Access*, Vol. 7, 563–586, 2018.
17. Remski, R., "Analysis of photonic bandgap surfaces using Ansoft HFSS," *Microwave Journal*, Vol. 43, No. 9, 190–199, 2000.
18. Pozar, D., "Input impedance and mutual coupling of rectangular microstrip antennas," *IEEE Trans. Antennas Propag.*, Vol. 30, No. 6, 1191–1196, 1982.
19. Pozar, D. and D. Schaubert, "Analysis of an infinite array of rectangular microstrip patches with idealized probe feeds," *IEEE Trans. Antennas Propag.*, Vol. 32, No. 10, 1101–1107, 1984.
20. Steyskal, H. and J. S. Herd, "Mutual coupling compensation in small array antennas," *IEEE Trans. Antennas Propag.*, Vol. 38, No. 12, 1971–1975, 1990.
21. Bhavarthe, P. P., S. S. Rathod, and K. T. V. Reddy, "Mutual coupling reduction in patch antenna using electromagnetic band gap (EBG) structure for IoT application," *Proc. IEEE International Conference on Communication Information and Computing Technology (ICCICT)*, 1–4, Mumbai, India, 2018.
22. Yang, F. and Y. Rahmat-Samii, "Microstrip antennas integrated with electromagnetic band-gap (EBG) structures: A low mutual coupling design for array applications," *IEEE Trans. Antennas Propag.*, Vol. 51, No. 10, 2936–2946, 2003.
23. Bhavarthe, P. P., S. S. Rathod, and K. T. V. Reddy, "A compact dual band gap electromagnetic band gap structure," *IEEE Trans. Antennas Propag.*, Vol. 67, No. 1, 596–600, 2019.
24. Park, J. D., M. U. Rahman, and H. N. Chen, "Isolation enhancement of wide-band MIMO array antennas utilizing resistive loading," *IEEE Access*, Vol. 7, 81020–81026, 2019.
25. Rahman, M. U., D. S. Ko, and J. D. Park, "A compact multiple notched ultra-wide band antenna with an analysis of the CSRR-TO-CSRR coupling for portable UWB applications," *Sensors*, Vol. 17, No. 10, 1–13, 2017.

26. Rahman, M. U., M. N. Jahromi, S. S. Mirjavadi, and A. M. Hamouda, "Bandwidth enhancement and frequency scanning array antenna using novel UWB filter integration technique for OFDM UWB radar applications in wireless vital signs monitoring," *Sensors (Basel)*, Vol. 18, No. 9, 1–14, 2018.
27. Rahman, M. U., M. N. Jahromi, S. S. Mirjavadi, and A. M. Hamouda, "Compact UWB band-notched antenna with integrated bluetooth for personal wireless communication and UWB applications," *Electronics*, Vol. 8, No. 2, 1–14, 2019.
28. Blanch, S., J. Romeu, and I. Corbella, "Exact representation of antenna system diversity performance from input parameter description," *Electron. Lett.*, Vol. 39, No. 9, 705–707, 2003.
29. Suntives, A. and R. Abhari, "Miniaturization and isolation improvement of a multiple-patch antenna system using electromagnetic bandgap structures," *Microw. Opt. Technol. Lett.*, Vol. 55, No. 7, 1609–1612, 2013.
30. Yu, A. and X. Zhang, "A novel method to improve the performance of microstrip antenna arrays using a dumbbell EBG structure," *IEEE Antennas Wireless Propag. Lett.*, Vol. 2, 170–172, 2003.
31. Maddio, S., G. Pelosi, M. Righini, S. Selleri, and I. Vecchi, "Mutual coupling reduction in multilayer patch antennas via meander line parasites," *Electron. Lett.*, Vol. 54, No. 15, 922–924, 2018.
32. Farahani, H. S., M. Veysi, M. Kamyab, and A. Tadjalli, "Mutual coupling reduction in patch antenna arrays using a UC-EBG superstrate," *IEEE Antennas Wireless Propag. Lett.*, Vol. 9, 57–59, 2010.
33. Xu, H. X., G. M. Wang, and M. Q. Qi, "Hilbert-shaped magnetic waveguided metamaterials for electromagnetic coupling reduction of microstrip antenna array," *IEEE Trans. Magn.*, Vol. 49, No. 4, 1526–1529, 2013.
34. Zheng, Q. R., Y. Q. Fu, and N. Yuan, "A novel compact spiral electromagnetic band gap (EBG) structures," *IEEE Trans. Antennas Propag.*, Vol. 56, No. 6, 1656–1660, 2008.